IEEE Transactions on Nuclear Science, Vol. NS-26, No. 3, June 1979

MEASUREMENTS OF SUPERCONDUCTING NIOBIUM CAVITIES AT 700 MHz

K. Yoshida+, M. Yoshioka+, J. Halbritter
Kernforschungszentrum Karlsruhe, Institut für Kernphysik II, Postfach 3640, 7500 Karlsruhe
Federal Republik of Germany

Abstract

Niobium TM_{010} cavities of different accelerating gap, but identical field emission geometries, were studied at 0.7 GHz. The measurement of $Q_0(E_p)$-depressions x-rays and electrons produced at high E_p-fields show enhanced field emission (FEM). This FEM loading depends on accelerating gap due to electron trajectories and impact generating slow (TSE) and fast (BSE) secondary electrons. In wide gap ($d_g \approx c/2f$), oxide coated Nb cavities enhanced FEM produce BSE which in crossing the gap drain energy out of the rf field. This limits the field already at $E_p \approx 10^7$V/m (f/GHz). Hidden in this FEM-BSE loading one side multipactor trajectories of second order at B_p=10mT have been identified, which were fed by FEM electrons and could be overcome.

I. Introduction

For a better performance of high energy storage rings, superconducting rf cavities at about .5 GHz are developed. [1] The rf cavities used for the acceleration of such fast particles are TM_{010} modes with a gap d_g of about c/2f. Nb cavities of this size are plagued by electron loading. For the highest fields reached $E_p \approx 10^7$V/m (f/GHz), the electron loading depends like field emission (FEM) on the electric field, i.e. [2-4] $j_e \propto \exp(-c/\beta E_p)$, where the "field enhancement factor" β is used as fit parameter using 4eV as work function. For Nb cavities the frequency and shape dependence [2-4] of β shows, that β is influenced by effects [5] in additon to a geometric electric field enhancement. To study this FEM type electron loading for 0.7 GHz Nb cavities, several cavities with identical FEM configuration but different gap length (2,11,12 and 22cm) have been studied below 4.2K. To analyze the limitations, the following diagnostic methods have been used:

- changes of $Q_0(T)$ with E_p
- local measurements of the x-ray spectrum
- electron current measurements by pick-up probes
- heat pulse measurements with carbon resistors
- electron trajectory computations.

The Q_0-values reached up to 10^{10} at 1.8K (R_{res}= 0.2nΩ) and changed only negligibly between 4.2 and 1.8K. In Table I the limiting FEM loading is summarized.

TABLE I
Typical results reached in oxide coated Nb cavities (TM_{010} mode at 0.7GHz). E_p^{max} occurs at r = 2.9 cm.

iris cavities	slotted	short	slotted	long
gap/(cm)	2	11	12	22
E_p^{max}/(MV/m)	∿16	5-6	5.5-6.5	6-7
β	280-660	650-1350	750-1200	660-1100

For wide gap cavities ($d_g \geq 11$cm), the loading is dominated by retarded FEM, which generate BSE crossing the gap and yielding a homogeneous impact at the endplates. Because η(BSE) is fairly independent of impact energy, i.e. on E_p, the very strong electron loading encountered, is due FEM. Such rapidly increasing FEM currents have never been observed for dc fields, but seem typical for rf fields in oxide coated Nb cavities at Helium temperature.

II. Experimental set-up

A schematic view of the experimental set-up is shown in Fig. 1. Q_0 and field strengths E and B are

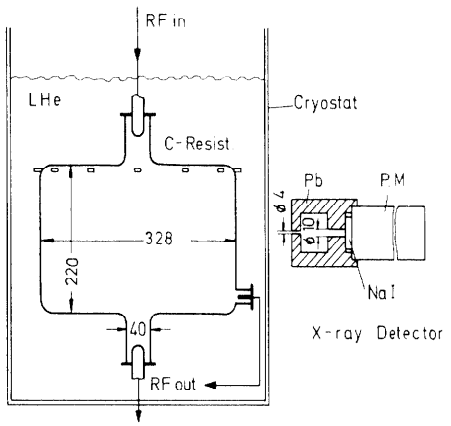

Fig. 1: Sketch of the experimental set-up for the long 700 MHz cavity

determined from the measurement of the rf power by the movable input coupling in the beam hole and by fixed coupling probes in the beam hole or in the hole at the corner. [7,8] The measurement of the bremsstrahlung x-rays was carried out in intensity and energy at various positions outside the cryostat by using a NaI scintillation counter with 2 Pb collimators. The spatical resolution of this detection system is ±2.7cm in 0.5m distance from the Nb cavity. The energy resolution and the channel (2keV) energy relation were calibrated using γ or β rays from radioisotopes. The energy resolution was found to be 25% for 511 keV βrays from Na [22]. In the present experiment, the energy ε_γ was defined as the x-ray energy corresponding to the channel where the counts have fallen to half of the maximal counts per channel. The x-ray yield I_γ is defined as this maximal counts times ε_γ. From the x-ray data the current of the impinging electrons can be deduced taking the shielding factors of the cavity wall and cryostat and all the x-ray efficiencies for the detector into account [7]. The dc current for various bias voltages between rf probes and cavity was measured with an accuracy of $\pm 10^{-9}$A. Bubbles of LHe caused by the rf breakdown at 4.2K were detected by 12 carbon thermoresistors, which were located with equal spacings at the upper corner of the cavity (Fig. 1). The location of the breakdown was determined from the time delay between the resistor signal and the rf breakdown. The Nb cavities were built from reactor grade Nb (Stanford specification) by Siemens (Erlangen) [8] or Leybold Heraeus (Hanau). Various surface treatments like: chemical polishing, electropolishing, UHV-firing and oxipolishing have been applied. FEM loading was changed in both directions, by rf-conditioning at a He-pressure of about 10^{-6}Torr.

III. Experimental Results

The experimental results typically show $Q_0(1.8K) \approx 10^{10}$ ($R_{res} = 2 \cdot 10^{-8}\Omega$) and $Q_0(4.2K) \approx 10^9$, which allows save operation at 4.2K at the field levels reached. Best results are usually obtained after a furnace treatment, but wet treatments yielding thicker oxides (≈5nm Nb_2O_5) [10] showed usually similar field strength but stronger FEM loading. Because of the

+ On leave of absence from Tykyo University

0018-9499/79/0600-4114$00.75 © 1979 IEEE

limited space we present results on the FEM loading of the long cavity only. The FEM loading enhances the rf losses as demonstrated in Fig. 2 and these losses are

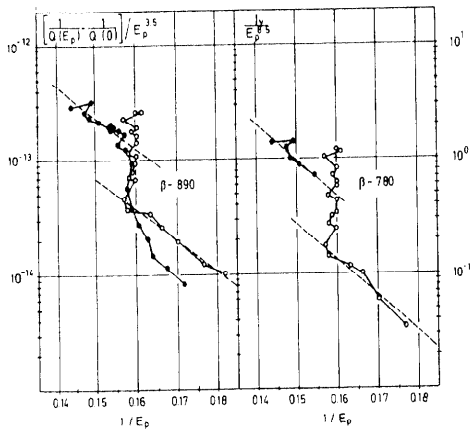

Fig. 2: Plots of $\Delta[1/Q(E)]/E^{3.5}$ and $I_\gamma/E^{8.7}$ for the long cavity, where the exponent of E^n is given by the averaging or shielding. The black dots and open circles in these Fowler Nordheim plots are different runs of the long cavity.

mostly in high energy electrons as demonstrated by the proportionality of $\Delta[1/Q(E)]$ and $I_\gamma(E)$ in Fig. 2. Detailed efficiency calculation showed, that the electron currents evaluated from $I_\gamma(E)$ can quantitatively explain $\Delta[1/Q(E)]$ and agrees in field dependence well with the electron currents $I_e(E)$ measured in the beam holes as shown in Fig. 3. A direct proof of the small content of

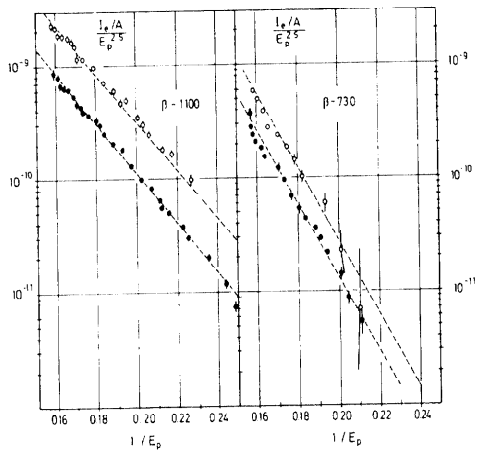

Fig. 3: Fowler Nordheim plots of the dc electron current at the rf input (left) and output (right) probes in the beam holes for the long cavity ∅: probe is positively biased with 180 V; ∅ without bias. The corresponding current density is given by $j_e/[A/cm^2] = \pi I_e$.

slow electrons in $j_e(E)$ is the observation, that growth of I_e with collecting voltage saturates in $I_e(U) \leq 2 I_e(0)$ already at 50V, where all slow secondaries get collected. This rapid increase of electrons loading the rf energy down is the actual limitation in field strength. In this FEM loading j_e jumps suddenly as shown in Fig.2, which also sometimes limits the E_p reached. These jumps around $E_p \simeq 6.4$MV/m are not caused by one side multipacting in corners, [5,6] which was found at $E_p \simeq 5.7$MV/m as peak in I_e from the corner probe plotted in Fig. 4. This peak at B_p=10mT is due to second order one side

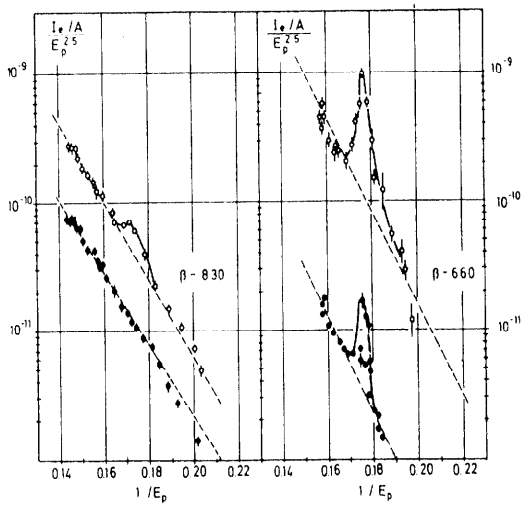

Fig. 4: Fowler Nordheim plots of the electron current in the hole in the corner of the long cavity for 2 different runs. The plot to the right corresponds to Fig. 3. The peak occurs at E_p=5.7MV/m which corresponds to B_p=10mT, i.e. B=8.7mT at the probe.

multipactor trajecties. [5,6,11] These trajectories seem fed by FEM electrons as shown in Fig. 4 by the higher peak for more background FEM electrons. The increase of $I_e(U)$ with collecting voltage U measured in the peak saturates around 100V, which indicates that the energies of electrons in the corner hole are below about 100eV. As shown in Fig. 4, the limit at $B_p \simeq 10$mT was overcome; only in one run at 4.2K rf breakdown was observed at this limit at the corner as detected by the carbon resistors.

To analyze the FEM loading further, the trajectories on which the electrons gain most of their energy have to be known. Informations about the trajectories can be obtained by I_γ and ε_γ at different positions, as shown in Fig. 5 and in Table 2.

TABLE 2

Current density $j_e(I_\gamma)$ deduced from x-rays for r>2cm, current density $j_e(I_e)$ measured in the coupling holes, mean impact energies ε_γ and integrated loading $\oint d_s j_e \varepsilon_\gamma$ in the different cavities

	E_p (MV/m)	j_e (I_γ) (nA/cm^2)	j_e (I_e) (nA/cm^2)	ε_γ (10^5eV)	P (Watt)
slotted iris: d_g=12cm	5.8	1.3	4.1*	3.3	0.3
	6.1	4.7	8.8*	3.4	1.2
long iris d_g=22cm	5.8	2.4	44***	2.7	1.1
	6.0	5.5	54***	2.8	1.7
	6.1	1.4	11*	2.6	0.37
	6.3	2.5	19*	2.7	0.69
	6.5	4.0	30*	2.8	1.14

* probe positively biased with 180 V
*** without bias

Fig. 5 indicates that for d_g=22cm I_γ and ε_γ do not vary much over the endplates, hinting to consecutive trajectories as cause for this FEM loading. Beside this electron cloud structure in the FEM loading appears as, e.g. the jumps in Fig. 2 or differences in β-values, e.g., in Figs. 2,3 and 4.

IV. Discussion

The above results of oxide coated Nb cavities (TM_{010} modes at 700 MHz) with identical FEM geometries show, that the ultimate field limitation is FEM loading

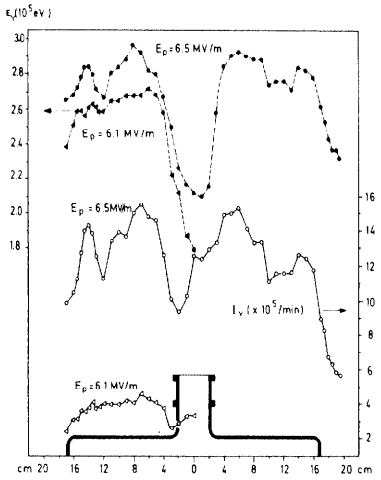

Fig. 5: X-ray distribution in intensity I_γ and energy ε_γ at the endplate of the long cavity at a field level E_p=6.1 and 6.5 MV/m

growing like exp(-c/βE). Although the FEM geometry is identical, the loading depends on cavity shape as summarized in Table 1. So, E_p is decreasing from 16 to 6.5 MV/m for d_g increasing from 2 to 22 cm while β is increasing from 300 to about 800. This geometry dependence indicates that trajectories are important for this loading, especially trajectories on which electrons gain more than .1MeV. Or, to be more accurate, we have to find an ensemble of trajectories, starting from FEM, which yield a flat I_γ - and ε_γ - distribution over the endplates and ε_γ(6.1MV/m)≃.26MeV and ε_γ(6.5MV/m)≃.29MeV. FEM electrons gain at 6.1MV/m between 50 and 170 keV, depending on retardation. [5] Thus, they are not able to explain ε≃.26MeV. But they produce secondaries - slow (TSE:ε<50eV) and fast [BSE:ε≃0.85 ε(impact)] ones. [12] For impact energies ε>50 keV, the yield η(TSE)<0.1 is small [12] and, in addition, it is unlikely that such TSE cross the gap gaining large amounts of energy. In contrast η(BSE)≃0.5 is fairly large [12] and such BSE easily cross the gap d_g∿22cm gaining so large amounts of energy (∿.6MeV), so that η(BSE)×.6MeV is still larger than ε_{FEM}≃.17MeV. Thus, the FEM loading in large rf cavities is qualitatively given by:

$$P \propto \exp(-c/\beta E_p)[\varepsilon_{FEM}+\eta(BSE)\varepsilon_{BSE}] \qquad (1)$$

$$\varepsilon_{FEM} \propto (E_p/f)^2; \quad \varepsilon_{BSE} \propto (E_p/f)$$

This model was worked out by computer simulation using retarded FEM smeared out in the high field region (2.7≤ r/cm≤3.3) and η(BSE,Nb)=.43. The resulting distribution of $I_\gamma(r)$ and $\varepsilon_\gamma(r)$ fits rather well Fig. 5. Even the enhanced current at the beam hole - see Table 2 - was reproduced in this simulation. According to Eq.(1), this simulation yields for any wide gap cavity (d_g∿c/2f) a mean energy $\varepsilon_\gamma \propto (E/f)$ and fairly homogeneous impact of electrons at the endplates, with some enhancement of j_e in the beam hole depending on d_g and gap shape. This scaling of ε_γ is confirmed by the agreement of ε_γ(0.7GHz, 6.1MV/m)=.26 MeV and ε_γ(1.2GHz, 10MV/m)=.26MeV rather well. [4] Also the fairly homogeneous impact was reproduced at 1.2GHz. So this type of combined FEM-BSE loading seems to be the ultimate limit in wide gap (∿c/2f) cavities. In the GHz range [2-5] this limit seems to follow

$$E_p^{max} \simeq 10^7 \text{ V/m (f/GHz)} \qquad (2)$$

A slightly lower limiting field was found for d_g=11 and 12 cm, where electrons on 1st order 2 side multipactor trajectories can cross the gap and can gain about .32MeV at 6.1MV/m. This energy ε_γ and the corresponding distribution [5] was found in our experiments [7]. The electron current j_e was fairly r - independent - see Table 2 - confirming that these trajectories are fed by FEM as above for d_g=22 cm. So geometry changes for d_g>c/8f, where most FEM hit the same surface, will change E_p only slightly According to [12], η(BSE) is constant above 10keV. Thus the field enhancement factors β are dominated by the field emission process and so we have to conclude, that rf field emission in oxide coated Nb cavities is geometry (Table 1) and frequency dependent $(\beta \propto f^{-1})^{2-5}$. The large β's can be explained by positive charging of the oxide by electron impact.[5] The d_g dependence (Table 1) hints to the fact that most positive charges have recombined after 1/2f, so that for d_g=2cm the FEM does not produce positive oxide charges at the right E-phase. The frequency dependence $^{2-4}$ of $\beta \propto f^{-1}$ could then be explained by retardation. [5] But more experiments are needed to clear the role of the oxide on the rf FEM.

One side multipactor trajectories of second order caused a peak in the electron current I_e in the corner at E_p=5.7MV/m. This peak seems fed by FEM electrons as indicated by a higher peak for a higher FEM background current in Fig. 4. The width of this peak, the position at B_p=10mT and the impact energies ε_e<100 eV estimated from $I_e(U)$ agree well with computer simulations made at Stanford for this geometry.[11] The yield enhancement factor [6] at 10mT was computed to be 1.7. In contrast to one side multipacting at higher frequencies $B_{pn}(f) \simeq 28mT/n(f/GHz)$ [5,6], we had at .7GHz no problem to overcome this limit at 10mT in our single cell cavity. The ease of overcoming multipactor level at lower frequencies seems to be due to the smaller rf losses skaling like $R(T)B_{pn}^2/2 \propto R(T)f^2$, which need for rf breakdown more impinging electrons than at higher frequencies. But our single cell cavity and good cooling may have helped also to overcome multipacting.

V. Conclusion

In line with other experiments on large gap oxide coated Nb cavities, the ultimate limit in E_p is set by field emission (FEM) charging the oxide and generating secondaries. The enhanced FEM by oxide charging seems crucial for the limitation encountered; but more experiments are needed to clarify this mechanism. The secondary electrons, especially the fast back diffused (BSE) ones, drain, in crossing the gap, most energy out of the rf field loading so the cavity down. 2nd order 1 side multipacting in this single cell 0.7GHz cavity was easily overcome.

Acknowledgement: The authors acknowledge the help of W. Bauer, H. Baumgärtner, U. Feißt, D. Hamdi, R. Lehm, K. Mittag, M. Rutz, F. Schürrer and R. Vincon. The computer simulation of 2nd 1 side multipacting was carried out by C.M. Lyneis (Stanford), whom we want to thank for his help very much.

References:

1 W. Bauer et al., this conference
2 C.M. Lyneis, M. McAshan, N.T. Viet, Proc. 1972 Proton Linear Acc. Conf., Los Alamos (LASL, 1972),p.98
3 P. Kneisel, O. Stoltz, J. Halbritter, J. Appl. Phys. 44, 1785 (1973) and J. App. Phys. 45, 2302 (1974)
4 I. Ben Zvi, J.F. Crawford, J.P. Turneaure, IEEE Trans. NS-20, 54 (1973)
5 J. Halbritter, KfK-Extern3/78-1(KfK,Karlsruhe,1978)
6 C.M. Lyneis, H.A. Schwettman, J.P. Turneaure, Appl. Phys. Lett. 31, 541 (1977)
7 M. Yoshioka, Primärberichte (Kernforschungszentrum Karlsruhe, 1979) unpublished
8 K. Mittag, IEEE Trans NS-24, 1156 (1977)
9 C.M. Lyneis, P. Kneisel, O. Stoltz, J. Halbritter, IEEE Trans MAG-11, 417 (1975)
10 M. Grundner, J. Halbritter, to be published
11 C.M. Lyneis, private communication
12 R. Kollath, Handbuch der Physik XXI (Ed. S. Flügge, Springer Verlag Berlin, 1956)